

## Comparison between OH\* Chemiluminescence and OH Planar Laser-Induced Fluorescence Images in a Light-Duty Optical Diesel Engine

M.K. Le<sup>1</sup>, S. Kook<sup>1</sup>, Q.N. Chan<sup>1</sup> and E.R. Hawkes<sup>2</sup>

<sup>1</sup>School of Mechanical and Manufacturing Engineering  
The University of New South Wales, New South Wales 2052, Australia

<sup>2</sup>School of Photovoltaic and Renewable Engineering  
The University of New South Wales, New South Wales 2052, Australia

### Abstract

Optical/laser-based imaging diagnostics have provided the science base needed by industry to develop new generations of high-efficiency, low-emissions diesel engines. Among others, OH\* chemiluminescence and OH planar laser-induced fluorescence (OH-PLIF) imaging are widely used to identify high-temperature reaction zones and their temporal evolution inside the engine cylinder. This study compares line-of-sight-integrated OH\* chemiluminescence images and multi-plane OH-PLIF images obtained in an automotive-size optical diesel engine. The results show that the OH\* signals generally match with the vertically integrated OH-PLIF signals for various crank angle locations. Also it is found that each imaging diagnostic has its own pros and cons. OH\* chemiluminescence imaging is easy to set up and effective in providing a temporal evolution of diesel flames. However, the line-of-sight-integrated image misses details of turbulent flame structures and can be affected by broadband emissions. On the other hand, the OH-PLIF signals are free from the bias caused by out-of-plane emissions and can display turbulent flame structures in higher details. Nevertheless, interference signals from fuel, PAH, or soot as well as laser beam attenuation can be problematic in the OH-PLIF imaging.

### Introduction

Optical/laser-based imaging diagnostics of diesel flames have been widely used to obtain a fundamental understanding that can help improve diesel engine combustion for lower levels of emissions [1-3]. One of the most common optical diagnostic techniques applied to diesel engines is OH\* chemiluminescence imaging [4-10]. This imaging technique captures the signals (306~310 nm) from naturally excited OH\* radicals when they return to the ground state [4, 5]. It is relatively easy to set up and useful to identify high-temperature reaction zones of diesel flames [5] as well as to determine key parameters such as the flame lift-off length [6-8]. However, being line-of-sight-integrated images, the structural details of diesel flames cannot be visualised. There are also many cases that ground-state OH signals are preferred (such as for computational modelling) over excited OH\* signals, particularly late in the combustion cycles with weak signals [2, 12, 13].

Planar laser-induced fluorescence of hydroxyl (OH-PLIF) is capable of visualising all ground-state OH radicals during diesel combustion [12-17]. This imaging technique detects the fluorescence signals emitted when OH radicals excited by a high-energy laser beam return to their ground state [18, 19]. The tomographic imaging of OH-PLIF helps extract the structural information within the flame. OH-PLIF is often applied to the mixing-controlled combustion phase at which the reaction is not as intense and fast as the premixed combustion phase [2, 13, 14]. While providing detailed information about turbulent diesel

flames, the interference signals from other fluorescence sources (e.g. fuel or PAH: polycyclic aromatic hydrocarbon) as well as soot incandescence signals are problematic [15, 16]. Therefore, low-sooting fuels are widely used together with series of optical filters [14, 15, 17]. Also, a comparison between online and offline OH-PLIF images are commonly applied given that the OH fluorescence absorptions and emissions change drastically with very small difference in the excitation wavelength. This is due to its well-defined, fine-scale rotational-vibrational structure [18, 19]. By comparing images taken under the wavelength tuned on and off to the OH excitation fluorescence line, the location and intensity of the interferences can be identified. This method is particularly useful for a high-sooting conventional diesel fuel.

This study compares these two diagnostics applied to the same target diesel flame in a small-bore optical diesel engine. Both OH\* chemiluminescence and OH-PLIF imaging have been performed for a single diesel flame under the influence of flame-wall interactions. The images were taken for various crank angle locations for the temporal evolution of the diesel flame. Also, the OH-PLIF imaging was performed for various distances below the cylinder head at two different laser wavelengths for online and offline signals.

### Experimental Setups and Diagnostics

#### Engine Setup and Operating Conditions

Experiments were carried out in a single-cylinder, light-duty, optical diesel engine. A schematic of the engine and the imaging

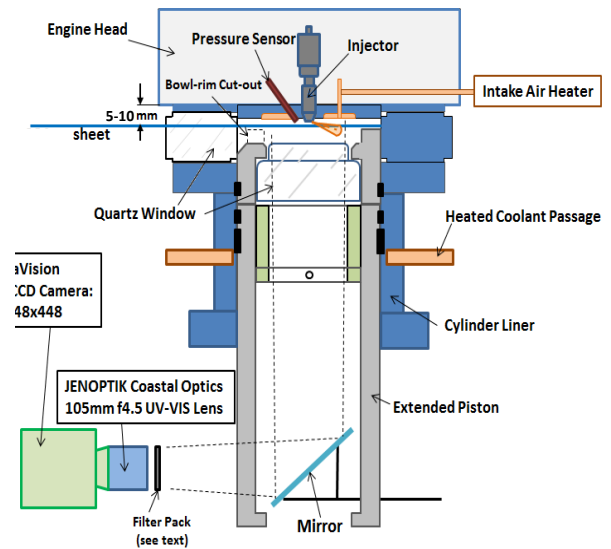


Figure 1. Schematic diagram of the optical diesel engine and laser diagnostic setup

diagnostics setup are shown in figure 1. The engine specifications and the selected operating conditions are summarised in table 1.

As illustrated in figure 1, the piston top and cylinder liner walls were replaced with quartz windows for optical access. For the bottom-view imaging, a 45° mirror was placed inside the extended piston body that was essentially a hollow cylinder. A portion of the piston bowl-rim (left-side in figure 1) was removed to allow an optical pathway for laser insertion even when the piston is at the vicinity of top dead centre (TDC). The original injector had seven 134- $\mu\text{m}$  holes. This was modified so that only one nozzle is left open by laser-welding the other six holes. The single-hole approach allowed for long injection duration that effectively caused flame-wall interactions while the injection still occurs. The injection duration of 2.36 ms (actual) at 70 MPa corresponded to 10 mg of fuel mass per injection. This injection mass was applicable to high-load engine conditions if all seven holes were considered. The single-hole nozzle was also useful to isolate the target fuel jet from complex jet-jet interactions. The engine was run by an AC motor at fixed speed of 1200 rpm and skip-fired (1 in 10 injection) for minimal residual gases from the previous firing cycle and avoid heavy thermal loading on quartz windows. The injection timing was fixed at 7 crank angle degrees before TDC ( $^{\circ}\text{CA bTDC}$ ).

#### In-cylinder Pressure and Apparent Heat Release Rate

As shown in figure 1, a piezoelectric pressure transducer (Kistler 6056A) was installed on the cylinder head to measure the in-cylinder pressure. The pressure traces were ensemble-averaged over 20 firing cycles. The apparent heat release rate was derived from the in-cylinder pressure data using a simple energy balance [19].

#### OH\* Chemiluminescence

OH\* chemiluminescence signals were captured using an intensified charge-couple device (ICCD) camera (LaVision

NanoStar) equipped with a UV-enhanced 105 mm f/4.5 lens (CoastalOpt®). The imaging setup is shown in figure 1. To isolate the emission range of OH\* chemiluminescence, optical filters including a WG305 glass filter and a 300 nm band-pass filter (FWHM: 40 nm, 70% maximum transmission) were placed in front of the ICCD camera lens. At each crank-angle location, a total of 20 images were taken from 20 firing cycles.

#### OH-PLIF

A Rhodamine-6G filled dye laser (Sirah Cobra-Stretch) was pumped by a frequency doubled beam (532 nm) from an Nd:YAG laser (Quanta-Ray Pro-230) to produce the desired OH-PLIF excitation wavelength of 284 nm. The optical filters of OH\* chemiluminescence imaging was used again to reject scattering light from the excitation laser and to block some broadband emissions. The same ICCD camera and lens were used. The emitted laser beam was converted to a 30-mm wide and roughly 300- $\mu\text{m}$  thick laser sheet before being inserted into the combustion chamber through the cylinder liner quartz window. The OH-PLIF imaging was performed for three different horizontal planes that were 5, 7 and 10 mm below the cylinder head. The signal interference issue was addressed by using 284 nm laser beam for “online” OH-PLIF imaging and 283.9 nm laser beam for “offline” OH-PLIF imaging. For the comparison purposes, the boundaries of the offline signals were overlaid on the corresponding online OH-PLIF image. It should be noted that the images presented in the following section are not ensemble averaged but selected individual cycles in order to retain turbulent flame structures. A correlation coefficient-based selection protocol was used for the selection; it chose the instantaneous cycle image that resembled the ensemble averaged image the most and hence, best represent the entire image set. For consistency, the same selection method was applied to OH\* chemiluminescence images. Details about this selection method are found in previous studies [16, 20].

#### **Results and Discussions**

Figure 2 displays the in-cylinder pressure trace (top) and apparent heat release rate (bottom) for the selected conditions of this study. The period of interest is annotated by “A” in the graphs, which is from around 9.5 $^{\circ}\text{CA aTDC}$  to the peak of the aHRR at 13 $^{\circ}\text{CA aTDC}$ . This is where the in-cylinder pressure of the firing cycles start to depart from the motoring pressure trace (non-firing cycles), which is commonly regarded as the start of combustion in a diesel engine. The steep increase in aHRR occurs at around 9 $^{\circ}\text{CA aTDC}$  when the mixtures formed during the ignition delay burn rapidly (i.e. premixed combustion phase). The comparison between OH\* chemiluminescence and OH-PLIF was made for this period as this is when OH\* concentration is at its maximum.

Figure 3 (leftmost column) shows the OH\* chemiluminescence (false coloured cyan) captured at 9.5, 11.5, 12.5 and 14.5 $^{\circ}\text{CA aTDC}$ . Also shown in figure 3 next to the OH\* chemiluminescence images are the corresponding offline and online OH-PLIF images (false coloured yellow for offline OH-PLIF signal and blue for online OH-PLIF signal) with the laser sheet placed 7 mm below the cylinder head.

The figure shows that the OH\* chemiluminescence signals appear first in the wall-jet head region before expanding back towards the jet-wall impingement point. Also, the right side of the wall-interacting jet shows stronger and larger OH\* chemiluminescence. This was explained by the swirl flow in the clockwise direction (swirl ratio = 1.4, see table 1) that caused richer mixtures and lower scalar dissipation rates on the down-swirl side of the fuel jet [20, 21]. The offline/online OH-PLIF images, however, show a different trend to OH\* chemiluminescence images. For example, at 9.5 $^{\circ}\text{CA aTDC}$  when the fuel injection still occurs, offline OH-PLIF signals are nearly

<b>Displacement (single-cylinder)</b>	497.5 cm <sup>3</sup>
<b>Bore</b>	83 mm
<b>Stroke</b>	92 mm
<b>Compression ratio (geometric)</b>	15.2
<b>Swirl ratio</b>	1.4
<b>Wall (coolant) temperature</b>	363 K
<b>Intake air temperature</b>	303 K
<b>Fuel</b>	Ultra low sulphur diesel (Cetane:51)
<b>Injector type</b>	Second-generation Bosch common-rail
<b>Nozzle type</b>	Hydro-grounded, K1.5/0.86
<b>Nozzle diameter</b>	134 $\mu\text{m}$
<b>Included angle</b>	150 $^{\circ}$
<b>Number of holes</b>	1
<b>Rail pressure</b>	70 MPa
<b>Injection duration</b>	2.36 ms
<b>Injected fuel mass</b>	10 mg
<b>Injection timing</b>	7 $^{\circ}\text{CA bTDC}$
<b>Engine speed</b>	1200 rpm

Table 1. Engine specifications and operating conditions

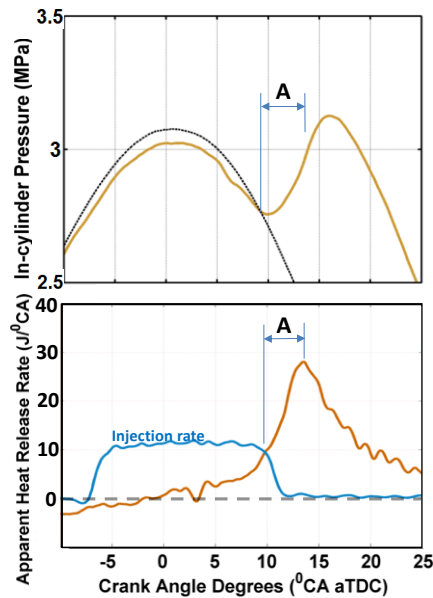


Figure 2. In-cylinder pressure trace for motoring (black dot line) and firing (brown solid line) cycles shown at the top and the apparent heat release rate (aHRR) trace at the bottom. Also shown is the measured fuel injection rate (blue solid line). The time period for OH-PLIF and OH\* chemiluminescence imaging is annotated by “A”.

identical to online OH-PLIF signals, suggesting that the fluorescence signals at this time are largely dominated by fuel fluorescence. There is also possibility that the up-swirl online signals are from the ground state OH produced from the decomposition of fuel molecules rather than the exothermic reactions releasing strong OH\* chemiluminescence [3].

At later crank angle locations, the OH\* chemiluminescence also develops on the up-swirl side of the jet while the down-swirl signals develop more intensely. This coincides with the online OH-PLIF signals that began to exceed the offline signals in both the strength and coverage area. When the down-swirl side of jet is closely looked at, the strong OH\* chemiluminescence signals exist in the same wall-jet head region of strong online OH-PLIF signals. Therefore, when the high-temperature reaction occurs actively, the OH\* chemiluminescence and OH-PLIF images show consistent trends in terms of the diesel flame development. At 12.5 and 14.5°CA aTDC, the offline OH-PLIF signals are very weak, suggesting no signal interference from fuel fluorescence. The offline OH-PLIF signals at this time are likely soot incandescence, implying that the soot pockets are trapped by OH.

While figure 3 shows an overall good match between OH\* chemiluminescence and online OH-PLIF images, many differences are also inevitable even at later crank angle locations

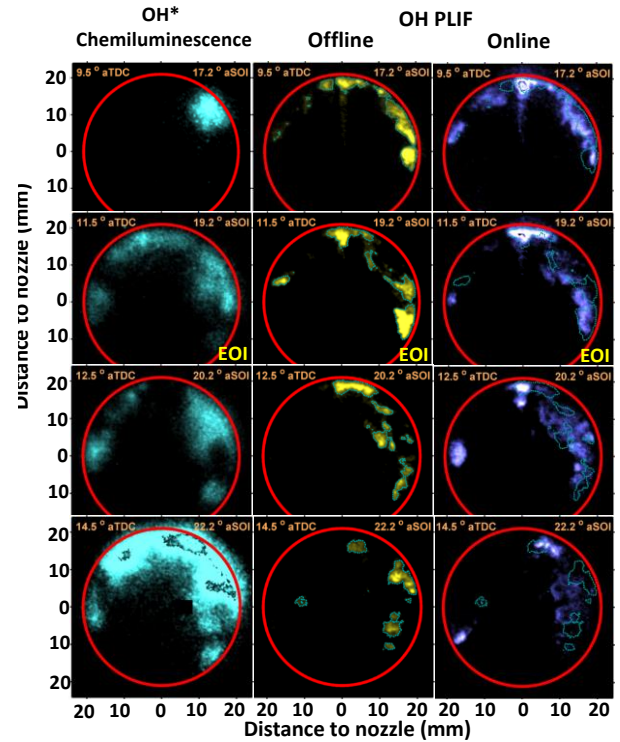


Figure 3. OH\* chemiluminescence images (left), offline OH-PLIF images (middle) and online OH-PLIF images (right) during high temperature reaction period. The PLIF images were taken at 7 mm below the cylinder head. The boundaries of offline images are overlaid on the online images for comparison. EOI denotes the end of injection.

with minimal fuel fluorescence. For example, the strong OH\* chemiluminescence on the up-swirl side is not found in the online OH-PLIF images. Some signals with an isolated island shape appears at 12.5 and 14.5°CA aTDC in the 9 o'clock direction, which however is not consistent with the strong OH\* chemiluminescence signals at the same crank angle location. This could be due to laser attenuation as some combustion gases might be in the way of the laser beam path. However, the mismatch could be simply due to the OH-PLIF image taken at a certain vertical distance from the cylinder head.

To address this issue, multiple horizontal planes at 5, 7 and 10 mm below the cylinder head were imaged for the online OH-PLIF signals. The results are shown in figure 4. The OH\* chemiluminescence images taken at the same crank angle location are also shown at the bottom of each image set for the comparison purposes. Visual inspection suggests that indeed OH\* chemiluminescence signals have a good agreement with the online OH-PLIF images when multi-plane signals are integrated. For example, the 5-mm plane image at 10.5°CA aTDC shows no

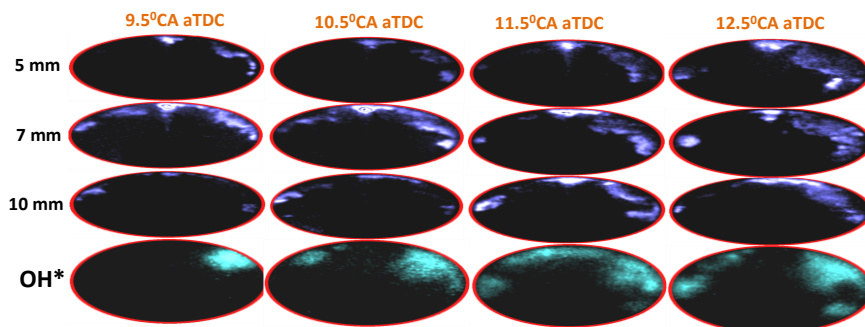


Figure 4. Online OH-PLIF images during high-temperature reactions at various distances from the cylinder head between 9.5 and 12.5°CA aTDC. Shown at the bottom are line-of-sight integrated OH\* chemiluminescence images.

OH signals on the up-swirl side although OH\* chemiluminescence signals do exist. It was because most of OH signals are found in lower planes (7 and 10 mm). Similarly, the OH signals at 5 and 7 mm at 11.5°CA aTDC are very weak but the strong signal is found in the 10 mm plane, which explains the OH\* chemiluminescence shown at the bottom. It should be noted that the up-swirl OH-PLIF signals at 9.5°CA aTDC was under the strong influence of fuel fluorescence as discussed previously.

### Conclusion

Two non-intrusive diagnostics, OH\* chemiluminescence and OH-PLIF were carried out in a single-cylinder, light-duty, optical diesel engine. The signals between the line-of-sight-integrated OH\* chemiluminescence and multi-plane OH-PLIF are compared to evaluate their pros and cons for the analysis of diesel flames. Major findings from this study are summarised as follows:

- The line-of-sight-integrated images from OH\* chemiluminescence is relatively easy to set up and useful to understand overall flame development flame structures. Since this diagnostic captures naturally excited OH\*, it is excellent in capturing the hot reaction zones and shows a good agreement with the high heat release rate. The drawback is that turbulent structures of diesel flames are smeared out in the OH\* chemiluminescence images.
- The OH-PLIF imaging visualise ground-state OH using external (laser) excitation source. The OH-PLIF signals are free from the out-of-plane emissions and can display the details of the turbulent structures of diesel flames. However, the signal interferences are significant, particularly from the fuel fluorescence and soot incandescence.
- When OH-PLIF images are taken for multiple horizontal planes from various distances below the cylinder head and compared to the line-of-sight-integrated OH\* chemiluminescence image, the signals match well for the overall flame development. However, the OH-PLIF images provide more details about the spatial distribution of OH signals in both horizontal and vertical directions.

### Acknowledgments

Experiments were conducted at the UNSW Engine Research Laboratory, Sydney, Australia. Support for this research was provided by the Australian Research Council.

### References

- [1] Dec, J.E., A Conceptual Model of DI Diesel Combustion Based on Laser-Sheet Imaging, *SAE paper 970873*; 1997.
- [2] Dec, J.E. & Tree, D.R., Diffusion-Flame/Wall Interactions in a Heavy-Duty DI Diesel Engine, *SAE paper 2001-01-1295*; 2001.
- [3] Musculus, M.P.B., Miles, P.C. & Pickett, L.M., Conceptual models for partially premixed low-temperature diesel combustion, *Prog. Energ. Combust.*, **39**, 2013, 246-283.
- [4] Higgins, B., McQuay, M.Q., Lacas, F., Rolon, J.C., Darabiha, N. & Candel, S., Systematic measurements of OH chemiluminescence for fuel-lean, high-pressure, premixed, laminar flames, *Fuel*, **80**, 2001, 67-74.
- [5] Dec, J.E. & Espey, C., Chemiluminescence Imaging of Autoignition in a DI Diesel Engine, *SAE paper 982685*; 1998.
- [6] Higgins, B. & Siebers, D., Measurement of the Flame Lift-Off Location on DI Diesel Sprays Using OH Chemiluminescence, *SAE Technical Paper 2001-01-0918*, 2001.
- [7] Pickett, L.M. & Siebers, D.L., Soot Formation in Diesel Fuel Jets Near the Lift-Off Length, *Int. J. Engine Res.*, **7**, 2006, 103-130.
- [8] Zhang, J., Jing, W. & Fang, T., High speed imaging of OH\* chemiluminescence and natural luminosity of low temperature diesel spray combustion, *Fuel*, **99**, 2012, 226-234.
- [9] Pickett, L.M., Siebers, D.L. & Idicheria, C.A., Relationship Between Ignition Processes and the Lift-Off Length of Diesel Fuel Jets, *SAE Paper 2005-01-3843*; 2005.
- [10] Polonowski, C.J., Mueller, C.J., Gehrke, C.R., Bazyn, T., Martin, G.C. & Lillo, P.M., An Experimental Investigation of Low-Soot and Soot-Free Combustion Strategies in a Heavy-Duty, Single-Cylinder, Direct-Injection, Optical Diesel Engine, *SAE Int. J. Fuels Lubr.*, **5**, 2011, 51-77.
- [11] Rusly, A.M., Le, M.K., Kook, S. & Hawkes, E.R., The shortening of lift-off length associated with jet-wall and jet-jet interaction in a small-bore optical diesel engine, *Fuel*, **125**, 2014, 1-14.
- [12] Musculus, M.P.B., Effects of the In-Cylinder Environment on Diffusion Flame Lift-Off in a DI Diesel Engine, *SAE Paper 2003-01-0074*; 2003.
- [13] Dec, J.E. & Coy, E.B., OH Radical Imaging in a DI Diesel Engine and the Structure of the Early Diffusion Flame, *SAE paper 960831*; 1996.
- [14] Musculus, M.P.B., Multiple Simultaneous Optical Diagnostic Imaging of Early-Injection Low-Temperature Combustion in a Heavy-Duty Diesel Engine, *SAE paper 2006-01-0079*; 2006.
- [15] Kashdan, J.T., Docquier, N. & Bruneaux, G., Mixture Preparation and Combustion via LIEF and LIF of Combustion Radicals in a Direct-Injection, HCCI Diesel Engine, *SAE Paper 2004-01-2945*; 2004.
- [16] Genzale, C.L., Reitz, R.D. & Musculus, M.P.B., Effects of Piston Bowl Geometry on Mixture Development and Late-Injection Low-Temperature Combustion in a Heavy-Duty Diesel Engine, *SAE Int. J. Engines*, **1**, 2008, 913-937.
- [17] Donkerbroek, A.J., van Vliet, A.P., Somers, L.M.T., Dam, N.J. & ter Meulen, J.J., Relation between hydroxyl and formaldehyde in a direct-injection heavy-duty diesel engine, *Combust. Flame*, **158**, 2011, 564-572.
- [18] McManus, K., Yip, B. & Candel, S., Emission and laser-induced fluorescence imaging methods in experimental combustion, *Exp. Therm. Fluid Sci.*, **10**, 1995, 486-502.
- [19] Heywood, J.B., Combustion in compression-ignition engines. *Internal combustion engine fundamentals*. New York: McGraw-Hill: 509-510, 1988.
- [20] Le, M.K., Kook S. & Hawkes, E.R., The planar imaging of laser induced fluorescence of fuel and hydroxyl for a wall-interacting jet in a single-cylinder, automotive-size, optically accessible diesel engine. *Fuel* (submitted June 2014)
- [21] Bruneaux, G., Mixing Process in High Pressure Diesel Jets by Normalized Laser Induced Exciplex Fluorescence Part II: Wall Impinging Versus Free Jet, *SAE paper 2005-01-2097*; 2005.